Motion of relativistic particles in standing-wave fields. II. Particles with spin

1979 J. Phys. A: Math. Gen. 12 2407

(http://iopscience.iop.org/0305-4470/12/12/019)

J. Phys. A: Math. Gen., Vol. 12, No. 12, 1979. Printed in Great Britain

Motion of relativistic particles in standing-wave fields II: Particles with spin

W Becker† and H Mitter‡

† Institut für Theoretische Physik der Universität, D-7400 Tübingen, West Germany
‡ Institut für Theoretische Physik der Universität, A-8010 Graz, Austria

Received 22 March 1979

Abstract. The Dirac equation in the presence of the classical field of a standing wave is investigated for an electron moving parallel to the beam direction. The main differences from the spinless case are: if the two plane waves which produce the standing wave have opposite polarisation, the energy bands for the two spin components are different; for the spin-averaged transmission coefficient this is of relevance only for very low energies; if the waves have equal polarisation, the momentum bands as found in the spinless case are completely absent.

1. Introduction

This paper continues an earlier one on the relativistic quantum mechanics of spinless particles in the classical field of a standing wave (Becker *et al* 1979b, to be referred to as I). We shall here consider spin effects on the basis of the Dirac equation. The investigation is motivated by the fact that one can not be at all sure that the pattern of the energy bands which has been discussed at length in I is not considerably altered by the electron spin. This is because both the appearance of energy bands and the consequences of spin are genuine quantum effects, both governed by the parameter $\hbar\omega$, ω being the frequency of the standing wave. Unfortunately the mathematical structure becomes much more involved if the spin is taken into account. Whereas we could use the elaborate theory of Mathieu's equation in the scalar case, we have to deal here with a first-order system of periodic differential equations, for which few exact results are known, especially for the required large parameter values involved. Apart from some general and qualitative statements, all results to be presented below will therefore be based on approximate solutions which are mostly obtained by numerical methods. Since the physical consequences are entirely different for equal and opposite polarisation, we shall treat the two cases separately.

2. Opposite polarisation

The Dirac equation for a particle in an external field A reads

$$[\gamma_\mu(\mathrm{i}\partial^\mu + \epsilon A^\mu) - \kappa]\phi(x) = 0 \tag{1}$$

(see I for the notation). With the vector potential of (I,equation (6)) the dependence on x, y may be split off as in I, equation (8) and we shall, as in I, equation (9), consider an

electron with canonical momentum along the z axis. The potential term in equation (1) can be written in the form

$$\epsilon\gamma_\mu A^\mu = -2i\epsilon a\rho_2\sigma_1 \cos \omega z S(2\omega x_0). \tag{2}$$

Here we have used Dirac's ρ and σ matrices

$$\gamma^0 = \rho_3, \qquad \gamma^k = \rho_3\rho_1\sigma_k, \qquad k = 1, 2, 3 \tag{3}$$

and the matrix for a spin rotation

$$S(\alpha) = \cos \alpha/2 - i\sigma_3 \sin \alpha/2. \tag{4}$$

Due to the invariance of the vector potential under the combined time translation and rotation around the z axis (I, equation (7)) we can separate the time dependence; things are only slightly more complicated than in the scalar case. With the ansatz

$$\phi(x_0, z) = \exp(-ip_0x_0)S(-\omega x_0)g(z) \tag{5}$$

we obtain a one-dimensional system of differential equations. In terms of the dimensionless quantities

$$\xi = \omega z, \qquad l = \epsilon\alpha/\omega,$$

(cf I, equations (11) and (13)) we have

$$[\mathrm{d}/\mathrm{d}\xi + i\rho_1/2 + \sigma_3(\rho_2\kappa - \mathrm{i}\rho_1 p_0)/\omega - 2l\sigma_2 \cos \xi]g = 0. \tag{6}$$

Iterating with the ansatz

$$g(\xi) = \rho_2\sigma_3[d/d\xi + \mathrm{i}\rho_1/2 - \sigma_3(\rho_2\kappa + \mathrm{i}\rho_1 p_0)/\omega - 2l\sigma_2 \cos \xi](1 - \mathrm{i}\rho_2)f(\xi) \tag{7}$$

we obtain the second-order system

$$[\mathrm{d}^2/\mathrm{d}\xi^2 + \Lambda_\sigma - 2l^2 \cos 2\xi + 2il\sigma_2\rho_3(\cos \xi - i\rho_3 \sin \xi)]f(\xi) = 0 \tag{8}$$

where we have

$$\Lambda_\sigma = (1/\omega^2)[(p_0 - \omega\sigma_3/2)^2 - \kappa^2] - 2l^2. \tag{9}$$

Comparison with I, equation (12) shows that the two spin components $\sigma_3 = \pm 1$ have different energies and remain coupled via the last term in equation (8).

Another useful form is obtained from equation (6), if we put

$$g_1 = h_1 + \mathrm{i}k_1, \qquad g_2 = \mathrm{i}(h_3 + \mathrm{i}k_3), \qquad g_3 = \mathrm{i}(h_4 + \mathrm{i}k_4), \qquad g_4 = h_2 + \mathrm{i}k_2. \tag{10}$$

Then we obtain two identical, real systems for the spinors h and k, which read

$$\mathrm{d}h/\mathrm{d}\xi = A(\xi)h \tag{11}$$

where

$$A(\xi) = \tfrac{1}{2}\mathrm{i}\sigma_1\rho_2 - \rho_1(\sigma_1\kappa/\omega + \mathrm{i}\sigma_2 p_0/\omega - 2l\sigma_3 \cos \xi). \tag{12}$$

The components of the current,

$$j^\mu = \bar{\phi}\gamma^\mu\phi, \tag{13}$$

read in terms of h

$$\begin{aligned} &j^0 = h^+h, \qquad j^3 = -h^+\rho_1\sigma_2 h \\ &j^1 \pm \mathrm{i}j^2 = -\mathrm{i}h^+\rho_1(\rho_3 \mp \sigma_3)h \exp(\mp \mathrm{i}\omega x_0) \end{aligned} \tag{14}$$

and current conservation

$$\partial_\mu j^\mu = 0$$

reduces to

$$\mathrm{d}j^3/\mathrm{d}\xi = 0. \tag{15}$$

As in the scalar case there are solutions of the Floquet type,

$$h(\xi) = \hat{h}(\xi)\exp(\mathrm{i}\tau\xi/2), \qquad \hat{h}(\xi+2\pi) = \hat{h}(\xi), \tag{16}$$

and the behaviour of the characteristic exponents is important. Some theorems, which are useful in this context, have been proved in a previous paper (Becker *et al* 1979a, to be referred to as II). Since the matrix (8) has the properties

$$A(\xi) = A^*(\xi) = A(-\xi) = -\rho_3 A(\xi)\rho_3$$

theorem 2 of II is applicable. Thus the four characteristic exponents can be grouped in complex conjugate pairs and in pairs of opposite sign. The sum of the exponents has to vanish, since $\mathrm{Tr}\,A = 0$. Therefore the set of characteristic exponents is $(\tau_1, -\tau_1, \tau_2, -\tau_2)$, with the three possibilities: (1) both numbers τ_1, τ_2 are real; (2) one of the numbers is real, one imaginary; (3) both numbers are imaginary. As in the scalar case we must have $j^3 = 0$ for any solution belonging to imaginary characteristic exponents and the charge density j^0 increases exponentially in this case. Therefore these solutions have no physical meaning. Thus the three possibilities given above define (1) allowed, (2) simply and (3) doubly forbidden domains in the space of parameters $(l, p_0/\omega)$ for given mass κ. This indicates that the propagation behaviour of the two spin components in the presence of a standing wave is different: none, one or both of them may be transmitted or reflected.

Figure 1, which is based on a numerical solution of equation (11), gives an impression of what happens in general. The values of the parameters are unrealistic and have been chosen for numerical convenience. The hatched areas are simply forbidden. There are two increasing and two bounded solutions corresponding to a pair of complex

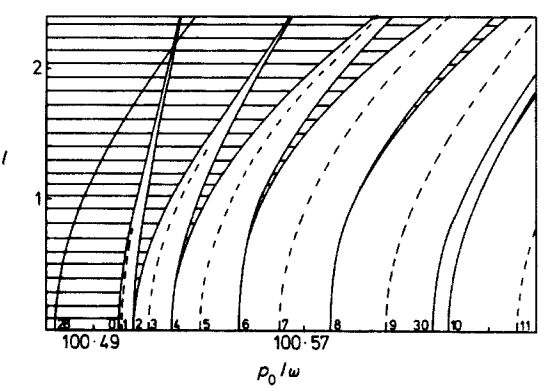

Figure 1. The stability chart of the system (11) for $\kappa/\omega = 100$. The hatched domains are simply forbidden. The only doubly forbidden domain which occurs in the figure is given by the intersection of the hatched areas with the apparent line $n = 28$. The indices of the characteristic curves are given at the abscissa. The disconnected curves correspond to odd integer values. There should be an additional disconnected curve with label $n = 29$ which is not depicted since it almost coincides with the band $n = 6$.

and a pair of real indices. Doubly forbidden domains are given by the intersection of the hatched areas with the apparent lines labelled $n = 28$ and $n = 30$. These lines actually represent extended simply forbidden domains which in the given scale shrink to lines. The labels n at the abscissa are the values of the characteristic index τ in agreement with equation (17) below. The lower values ($n = 0, 2, 4 \ldots$) correspond to the negative sign in (18), the upper values ($n = 28, 30$) to the positive sign.

If l is not too large, we can obtain the curves $\tau(l, p_0/\omega) = \text{constant}$ analytically by expanding the periodic function h in equation (16) in a Fourier series, inserting into equation (11) and evaluating the infinite determinant of the resulting system of equations for the Fourier coefficients to lowest non-trivial order in l (which is l^2). In this way we obtain

$$\tau_\pm/2 = B_\pm - l^2/B_\pm + O(l^4) \tag{17}$$

where

$$\omega B_\pm = [(p_0 \pm \omega/2)^2 - \kappa^2]^{1/2} \tag{18}$$

(this result is also valid for equal polarisation, if the sign of l^2 is changed and p_0 is replaced by p_z). From such a perturbative calculation τ results always as a real quantity. Since the eigenvalues $\exp i\pi\tau$ show continuity properties, τ can assume complex values only via a point, where τ is an integer. In fact, solving $\tau(l, p_0/\omega) = n$, $p_0/\omega = f_n(l)$ may yield two different curves $f_n(l)$, which then confine a region with non-real τ. Figure 1 shows that this happens for even, but not for odd, integer n (the disconnected lines are the graphs for $\tau = 2m + 1$). This fact has thus far been established only by numerical computation, where very narrow bands may be overlooked. The approximate investigation presented below indicates that this should hold also for the system (11).

Since the laser wavelength is large compared with the Compton wavelength of the particle, the energy splitting due to the spin is small. If we neglect the splitting term in equation (9) and write $F = (1 + i\sigma_1)f$, we obtain from equation (8)

$$[d^2/d\xi^2 + \Lambda - 2l^2 \cos 2\xi + 2il\sigma_3\rho_3(\cos\xi - i\rho_3 \sin\xi)]F = 0. \tag{19}$$

This is Mathieu's equation (I, equation (12)) supplemented by a term which describes a coupling of the two spin components. All possible choices $\rho_3 = \pm 1$, $\sigma_3 = \pm 1$ are equivalent upon $\xi \to \xi + \pi$ and/or $\xi \to -\xi$, so that we shall consider only $\rho_3 = \sigma_3 = 1$. With

$$G(\xi) = F(\xi) \exp(-2l \sin\xi)$$

we obtain a more convenient equation, which reads

$$G'' + 4l \cos\xi G' + (1 + 2l^2 + 2il \cos\xi)G = 0.$$

With a Floquet ansatz (16) we obtain a three-term recursion formula for the Fourier coefficients of the periodic part. The relation can be resolved in terms of continued fractions (Meixner and Schäfke 1954). The characteristic exponent is determined by a complicated equation, which we shall not write down here. With the exception of even integer values of τ a solution may be obtained by successive approximations. We obtain

$$\Lambda = \frac{\tau^2}{4} = 2l^4 \frac{\tau^2 - 13}{(\tau^2 - 1)(\tau^2 - 4)} + 2l^8 \frac{5\tau^8 - 491\tau^6 + 4251\tau^4 + 1159\tau^2 - 30844}{(\tau^2 - 1)^3(\tau^2 - 4)^3(\tau^2 - 16)} + \ldots \quad (\tau \neq 1)$$

$$\Lambda = \tfrac{1}{4} + 2l^2 \qquad (\tau = 1).$$

For large τ the leading terms in τ agree with those obtained from the corresponding expansions of equation (12) in I, if we identify $\tau/2$ as characteristic exponent according to the fact that the period of equation (12) in I is just half the period of equation (19). For even integer values of τ there are two solutions of the equation for $\Lambda(\tau, l)$, which branch at $\Lambda = \tau^2/4$, $l = 0$ and confine a region with complex τ. These solutions cannot be obtained by successive approximations.

Thus, although both the exact equations (11) and the approximative ones (19) for the spin-$\frac{1}{2}$ particle exhibit a period of 2π, whereas the equation (12) in I for the scalar particle has the period π, the qualitative picture of the allowed and forbidden domains is the same. For equation (19) the reason is that the forbidden domains start only at even integer values of τ. This latter fact may be understood also directly from equation (19): for small values of l we can neglect the third term; the resulting equation (for $\rho_3 = \sigma_3 = 1$) can be solved exactly in terms of Bessel functions

$$f \sim Z_\alpha\{(8l)^{1/2} \exp[-(i/2)(\xi + \pi/2)]\}, \qquad \alpha = (4\Lambda)^{1/2},$$

which are bounded for large $|\xi|$ for $\Lambda > 0$, so that there are no forbidden domains; thus the latter are due entirely to the term $l^2 \cos 2\xi$, as in the spinless case.

It has been pointed out in I that the energy bands are experimentally best observed near the classical threshold for transmission of particles. Hence the question arises, whether and how the transmission coefficient as plotted in I (figure 1) is modified due to the presence of spin. According to I, we need a very large value of l^2 for not-too-low values of the kinetic energy in order to reach the relevant region. Since we have found that the exact system of equations for spin-$\frac{1}{2}$ particles exhibits qualitatively the same pattern of allowed and forbidden domains as for spin-0, we can then (i.e. for $l^2 \gg l$) neglect the spin-coupling term in equation (8). Diagonalising σ_3 we obtain two Mathieu equations with different parameters Λ, i.e.

$$\Lambda_\sigma = \Lambda_\pm = (1/\omega^2)[(p_0 \pm \omega/2)^2 - \kappa^2] - 2l^2.$$

If we then compute the transmission coefficient with the Klein–Gordon theory as in I, we observe that the parameter on the abcissa of I (figure 1), has to be replaced according to

$$p = (1/\omega)(p_0^2 - \kappa^2)^{1/2} \to (p^2 \pm p_0/\omega + \tfrac{1}{4})^{1/2}.$$

For the uppermost graph of I (figure 1) (which is the most realistic one from the experimental standpoint) these mutual shifts of the scale are still small: the transmission coefficients for both spin components nearly coincide and the spin averaged coefficient is the same as in the spinless case. In the other two graphs neither is the shift small, nor can the neglection of the spin coupling be trusted. The spin effects will play a major role in this region, which is, however, experimentally hardly accessible because of the low kinetic energies involved.

3. Equal polarisation

With the vector potential of I, equation (50) the potential term in the Dirac equation (1) becomes

$$\epsilon\gamma_\mu A^\mu = -2i\epsilon a\rho_2\sigma_1 \cos \omega x_0 S(-2\omega z). \tag{20}$$

For a particle with canonical momentum along the z axis we can split off the dependence on z, putting

$$\phi(x_0, z) = S(\omega z)g(\eta)\exp(\mathrm{i}\, zp_z) \tag{21}$$

where $\eta = \omega x_0 + \pi/2$ in accordance with I, equation (53). Then we obtain the system

$$\mathrm{d}g/d\eta = A(\eta)g(\eta) \tag{22}$$

with

$$A(\eta) = \frac{\mathrm{i}}{2}\rho_1 - \mathrm{i}\rho_3\frac{\kappa}{\omega} - \mathrm{i}\rho_1\left(\frac{p_3}{\omega}\sigma_3 + 2l\sigma_1 \sin\eta\right). \tag{23}$$

It is observed that the matrix A is antihermitian:

$$A^+(\eta) = -A(\eta). \tag{24}$$

Therefore theorem 1 of II applies and we can conclude that the system (22) has only stable solutions without any band structure. The same conclusion can be drawn directly from current conservation, which amounts to

$$\mathrm{d}j^0/\mathrm{d}\eta = 0$$

if one observes that j^0 is positive, so that there can be no increasing solutions. In this respect the situation is completely different from the scalar theory, where we had found increasing solutions with $j^0 = 0$, indicating copious pair production from the vacuum. There may be pair production also in the Dirac theory; Fermi statistics, however, excludes an exponential increase in time. The situation resembles the corresponding one for a homogeneous, time-dependent electric field, where the probability for the presence of a pair oscillates in time for spin-$\frac{1}{2}$ and increases exponentially for scalar particles (Narozhnyi and Nikishov 1973).

4. Conclusions

These are the main differences between the results for spin-0 and spin-$\frac{1}{2}$:

(1) For opposite polarisation, the simple pattern of allowed and forbidden domains in the space of the two parameters, field strength and energy, is replaced by two such patterns corresponding to the two different spin orientations which overlap and form allowed, simply and doubly forbidden domains. It is remarkable that both patterns follow essentially the stability chart of Mathieu's equation. The 'grating' in the spin-$\frac{1}{2}$ case has double wavelength compared with the spinless case; hence one expects at first glance that the forbidden domains are more densely spaced. We have argued that this is effectively not the case. As to the experimental possibility of observing the energy bands by detecting transmission or reflection of an electron beam from the standing wave, spin does not play a major role except for very low kinetic energies. In the latter case, however, the spin-averaged transmission coefficient may be completely different from that for spin-0.

(2) For equal polarisation the momentum bands discussed in I disappear completely and we have everywhere just bounded solutions. The wavefunction within the momentum bands describes a situation with zero charge density and increases in space exponentially, thus allowing for copious pair production from the vacuum, which is forbidden in the spinor case due to Fermi statistics.

References

Becker W, Gesztesy F and Mitter H, 1979a *Lett. Math. Phys.*
Becker W, Meckbach R and Mitter H 1979b *J. Phys. A: Math. Gen.* **12** 799–809
Meixner J and Schäfke F W 1954 *Mathieu'sche Funktionen und Sphäroidfunktionen* (Berlin: Springer)
Narozhnyi N B and Nikishov A I 1973 *Zh. Eksp. Teor. Fiz.* 1965 862–74 (*Sov. Phys. JETP* **38** 427–32)